

Stress Distribution in Human Zygomatic Pillar Using Three-Dimensional Finite Element Analysis

Distribución de la Tensión en el Pilar Cigomático Humano
Usando Análisis de Elementos Finitos Tridimensional

Felippe Bevilacqua Prado*, Pedro Yoshito Noritomi**, Alexandre Rodrigues Freire*,
Ana Cláudia Rossi*, Francisco Haiter Neto*** & Paulo Henrique Ferreira Caria*

PRADO, F. B.; NORITOMI, P. Y.; FREIRE, A. R.; ROSSI, A. C.; NETO, F. H. & CARIA, P. H. F. Stress distribution in human zygomatic pillar using three-dimensional finite element analysis. *Int. J. Morphol.*, 31(4):1386-1392, 2013.

SUMMARY: This paper aimed to analyze stress distribution in human zygomatic pillar during masseter muscle contraction using three-dimensional finite element analysis. A three-dimensional model and hemi facial skull were produced based on CT-scan data. An adult male skull with structural anatomy integrity was used as model. Muscles forces were applied at origin of elevator muscles and supports was applied at the occlusal surfaces at first and second molars to simulate a masticatory load and stimulate the zygomatic pillar. Supports were applied to the occlusal contacts. Symmetry conditions were placed at the mid-sagittal plane. For the top and back cutting plane, constraints were used. Equivalent Von-Mises Stress and Maximum Principal Stress analysis were performed from the stress fields along the zygomatic pillar. It was represented by stress concentration at the alveolar process, zygomatic bone, frontal and temporal process of zygomatic bone and superciliary arch. Stress line indicates distribution of stress from maxilla toward the frontal and temporal bone. The stresses occurred due to resultant occlusal forces is mainly supported by the zygomatic bone, non-uniformly distributed and predominantly through the zygomatic pillar. This study contributed to better understanding of stress distribution in zygomatic pillar to understand the influence of chewing on zygomatic pillar morphology and also be useful for clinical practice.

KEY WORDS: Biomechanics; Skull; Finite element analysis.

INTRODUCTION

Craniofacial skeleton morphology reflects the functional demand. In the skull the masticatory mechanical loads are distributed in different directions (Hylander *et al.*, 1991; Ross, 2001; Cattaneo *et al.*, 2003; Hilloowala & Kanth, 2007; Strait *et al.*, 2009). This is one of the basic fundamentals of skull biomechanics.

This concept states that skull pillars are resistance areas adapted for functional and non-functional mechanical induction (Sicher & DuBrul, 1970; Hylander *et al.*, 1991). One of the most resistant areas of the skull involved in the distribution of stress from masticatory forces is the zygomatic pillar (ZP) (Hilloowala *et al.*).

Experimental strain gauges (Endo, 1965) and finite element analysis (FEA) in non-human primates (Kupczik *et*

al., 2007; Chalk *et al.*, 2011; Strait *et al.*, 2009, 2010) have improved our understanding about skull biomechanics and morphological adaptation related to feeding and evolution (Richmond *et al.*, 2005; Strait *et al.*, 2009; Wroe *et al.*, 2010). Additionally, FEA is an effective tool for applications on skull biomechanics that improves our understanding of how masticatory mechanical loads are distributed through skull (Turner, 1998; Huiskes & Chao, 1983; Pavalko *et al.*, 2003; Silva *et al.*, 2005; Kupczik *et al.*).

Skull biomechanics concepts should be applied in the different areas of dentistry (Shetty *et al.*, 2010; Prado *et al.*, 2013). Based on skull biomechanics concepts, the purpose of this study was to analyze stress distribution in human ZP during masseter muscle contraction using three-dimensional finite element analysis.

* Department of Morphology, Anatomy area, Piracicaba Dental School, State University of Campinas, Piracicaba, São Paulo, Brazil.

** Division of Three-dimensional Technologies, Center for Information Technology “Renato Archer”, Campinas, São Paulo, Brazil.

*** Department of Oral Diagnosis, Oral Radiology area, Piracicaba Dental School, State University of Campinas, São Paulo, Brazil.

MATERIAL AND METHOD

Geometry acquisition and finite element meshing. We selected a dry human skull without skeletal pathology. Local Research Ethics Committee approved this research (no.175/09).

Sequential CT images was performed in a DICOM format using a GE HiSpeed NX/i CT scanner (General Electric, Denver, CO, USA) in axial plane, with 0.25 mm slice thickness. The CT scans of the skull were transferred into InVesalius software (Center for Technology and Information “Renato Archer”, Campinas, Brazil), where the anatomical structures (bone and teeth) were segmented by thresholding and to create a hemi-facial stereolithographic model (STL) (Fig. 1A).

Subsequently this STL model was transferred to the CAD program Rhinoceros® 3D 5.0 NURBS Modeling for Windows (McNeel & Associates, USA) to create a solid geometry by STL converting approach (Sun et al., 2005) (Figure 1B).

Three-dimensional parts were exported as STEP format and imported into the FEA software ANSYS v14 (Ansys Inc., USA) for finite element mesh conversion (Fig. 1C). The mesh generation resulted in a total of 121,806 tetrahedral elements and 189,640 nodes. The mechanical properties for each material (Table I) were determined from values obtained in the literature.

Boundary and Loading conditions. Regarding to boundary conditions, symmetry condition was applied at the midsagittal plane (Figure 2A). At the top and back cutting plane, restraints were chosen to simulate the presence of rest of skull (Figure 2A). Fixed supports were applied to the occlusal surface of both first and second left maxillary molars (Fig. 2B).

The force of elevator muscles was applied to each muscle insertion area. The action of muscle forces and the support at molar occlusal surface was applied to simulate a forced molar occlusion condition.

Table I. Material properties of anatomical structures with Young's modulus and Poisson ratio values.

Anatomical structures	Young's Modulus	Poisson Ratio
Bone	14000*	0.3
Tooth	19600**	0.3

*= Wroe et al. (2010); **= Tanne et al. (1985).

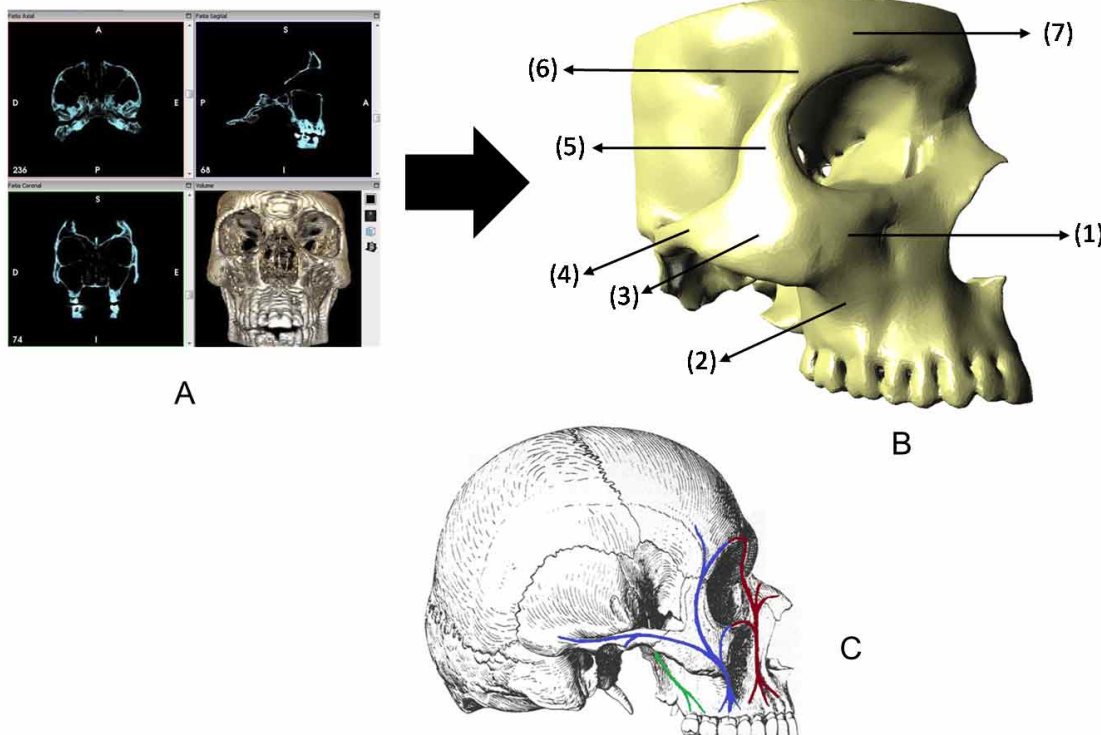


Fig. 1. Modeling process of 3D geometry of zygomatic pillar. A) Geometry acquisition from CT images. B) CAD model with the 7 regions along the zygomatic pillar. C) Load dissipation along the skull pillars. Blue line shows the force dissipation from molar biting (Modified from Sicher & Dubrul, 1970).

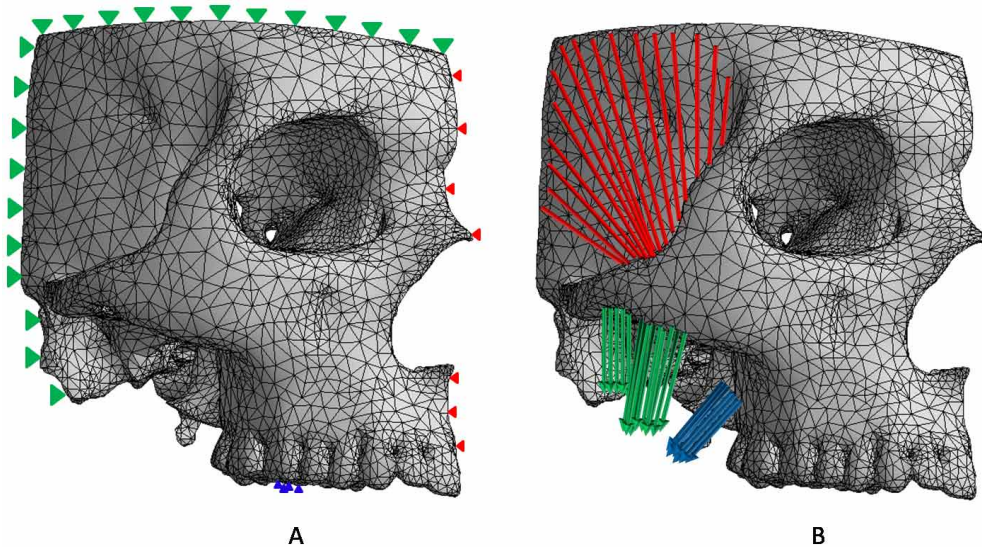


Fig. 2. Finite element mesh composed by tetrahedral elements. A) Boundary conditions: fixed support (blue), symmetry (red) and constraints (green). B) Muscular forces: temporal muscle (red), masseter muscle (green) and medial pterygoid muscle (blue).

RESULTS

Stress analysis was performed using the Equivalent Von-Mises Stress (VMS) and Maximum Principal Stress (MPS). Although the stress has distributed along the skull, the analysis of the VMS and MPS distribution was restricted to the ZP. Stresses were visualized using a color variation on the geometrical model.

To facilitate the understanding of the stress patterns along the zygomatic pillar, 7 points was defined and marked with the stress values (Table II). The 7 points was defined according the zygomatic pillar structures: 1) Zygomatic body; 2) Zygomatic alveolar crest; 3) Zygomatic body; 4)

Temporal process of zygomatic bone; 5) Frontal process of zygomatic bone; 6) Zygomatic process of frontal bone; 7) Superciliary arch.

Table II. Load magnitudes of human masticatory muscles* (N).

Muscle	Magnitude
Superficial masseter	190.4
Deep masseter	81.6
Temporal (anterior)	158
Temporal (middle)	95.6
Medial Pterygoid	174.8

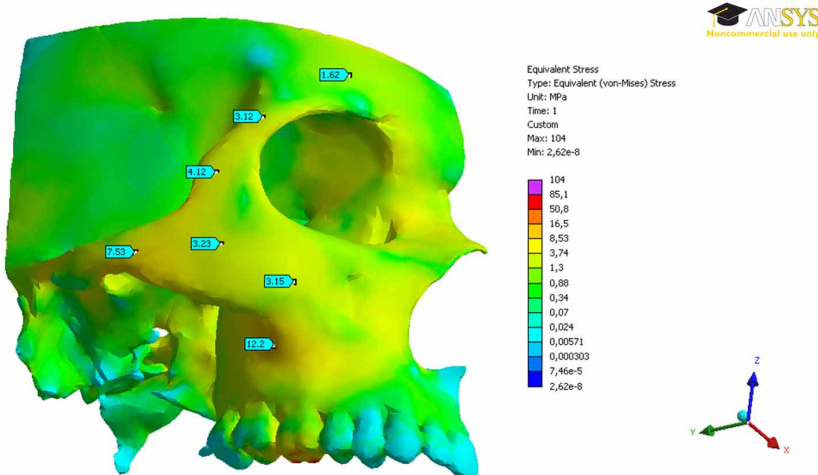


Fig. 3. Equivalent von-Mises stress from peak molar biting. High stress areas by yellow and orange colors and low stress areas by light blue and dark blue colors along the ZP. The 7 regions considered in this study were labeled with the stress values.

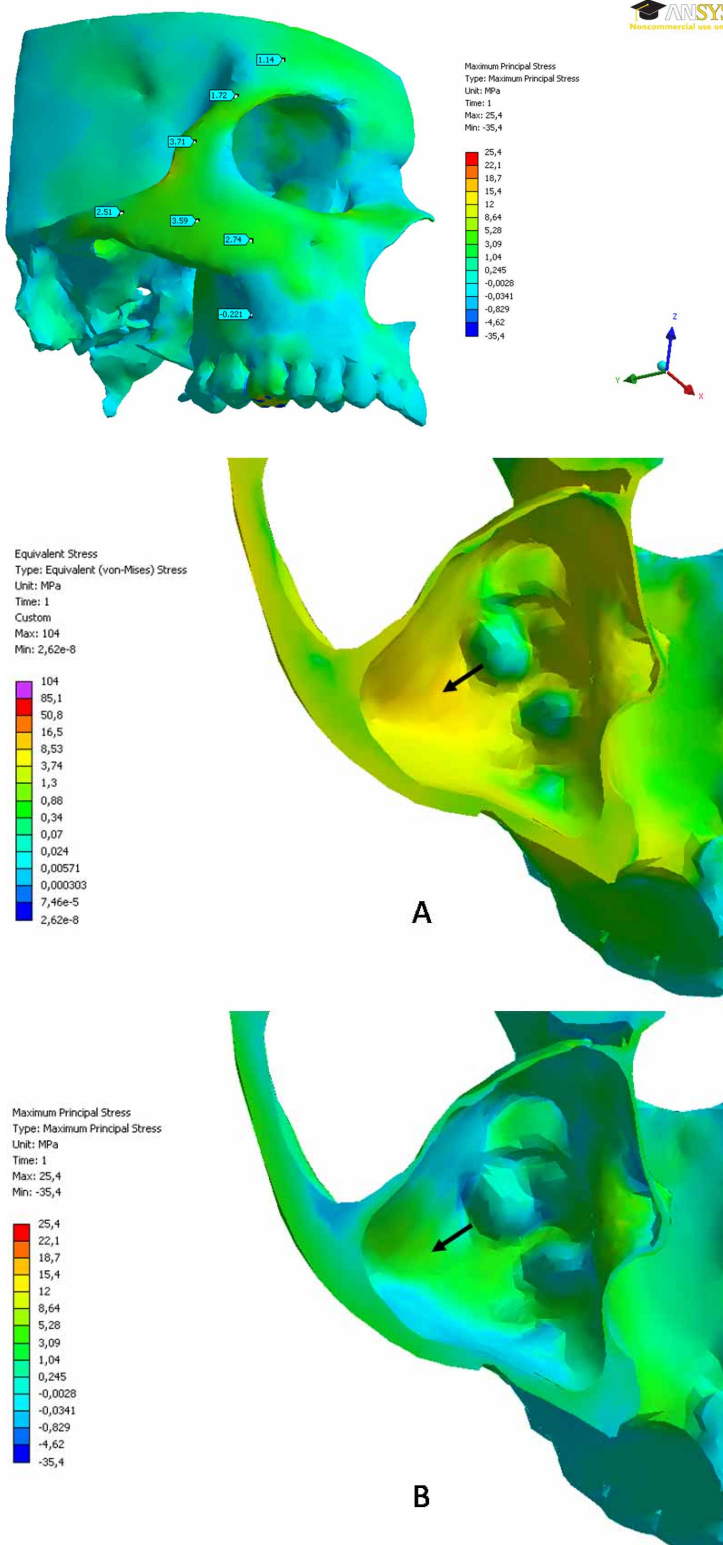


Fig. 5. Transversal section of skull model with internal view of maxillary sinus. A) Equivalent von-mises stress showed high stress at the lateral wall (indicated by the arrow). B) The high stressarea is characterized by tensile stress (indicated by the arrow).

Fig. 4. Maximum principal stress showing the tensile (positive) and compressive (negative) stress. The 7 regions considered in this study were labeled with the stress values.

Equivalent von-Mises Stress. The VMS (Fig. 3) showed distribution of stress on the alveolar process of maxilla and concentrated at the zygomatic alveolar crest (12.2 MPa), where also was observed at the lateral wall of maxillary sinus (Fig. 5). At the zygomatic bone the stresses occurred on the body and extended to the temporal process (3.23 and 7.53 MPa, respectively) and frontal process (4.12 MPa). At the zygomatic process of frontal bone occurred stress decrease near of the zygomatic frontal suture (3.12 MPa). On the superciliary arch the VMS was lower than other regions (1.62 MPa).

Maximum Principal Stress. The MPS (Fig. 4) showed compressive areas at zygomatic alveolar crest (-0.221 MPa).

In the zygomatic bone occurred tensile stress on the body (2.74 MPa) and temporal process (2.51 MPa). At the frontal process, occurred low compressive stress in a small area at the lateral margin of the orbit, but this process presented mainly tensile stress (3.71 MPa). The angle formed by the frontal process and temporal process presented a high tensile stress (12 to 15.4 MPa). At the zygomatic process of frontal bone the tensile stress decreased (1.72 MPa) and was the lower at superciliary arch (1.14 MPa).

At the maxillary sinus was observed a tensile stress on the floor and extended to the lateral wall (3.09 to 5.28 MPa) (Fig. 5).

Table III. Stress values (MPa) according the regions of structures that compose the zygomatic pillar.

Region	Equivalent von-Mises stress	Maximum principal stress
1	3.15	2.74
2	12.2	-0.221
3	3.23	3.59
4	7.53	2.51
5	4.12	3.71
6	3.12	1.72
7	1.62	1.14

DISCUSSION

Our study demonstrated the stresses distributed in human ZP by FEA. Some authors have shown areas of mechanical stress concentration during animal experiments (Hylander & Johnson, 2000; Herring, 2007) and strain gauges (Endo, 1966a, 1966b; Oyen *et al.*, 1996). Simulations by FEA of human and non-human primates (Strait *et al.*, 2009, 2010; Chalk *et al.*, 2011) involving masticatory mechanisms have also been resulted in reliable data.

A non-uniform stress distribution along ZP observed in our VMS results are similarly to the strain distribution results in early (Strait *et al.*, 2009) and modern human skulls (Wroe *et al.*). A non-uniform stress and strain distribution supports the discussion about the presence of resistance bone structures due to different non-mechanical factors (Hylander *et al.*, 1991), as spatial factors or secondary to sexual characteristics (Lanyon & Rubin, 1985). Thus, associated to previous FEA results (Strait *et al.*, 2009, 2010), the results of our study contributes to the hypothesis of variable environment of ideal deformations applied to the facial skeleton (Lanyon & Rubin, 1985).

Our VMS distribution presented stresses at the orbit contour, especially at the lateral margin and superciliary arch. We also observed MPS distribution of compressive areas at the lateral margin of the orbit (Fig. 4), similarly the results of strain gauges analysis by Endo (1966b). Although the present study showed stresses at the orbital region, the superciliary arch morphology is also influenced by spatial and allometric factors, i.e., orbit position related to the neurocranium. Moreover, superciliary arch morphology is related to the low frequency of traumatic and non-masticatory loads (Hylander *et al.*, 1991). Thus, our study demonstrated low value of VMS at the superciliary region in comparison to the zygomatic alveolar crest, characterizing the low mechanical influence by masticatory force in the superciliary morphology (Hylander *et al.*, 1991; Hylander & Johnson).

Application of mechanical loading resultant to the masseter muscle contraction showed two lines of tensile stress at the maxillary sinus walls. Sinuses wall are areas of compact bone (Blaney, 1990; Prossinger & Bookstein, 2003), located between the skull pillars (Endo, 1965; Preuschoft *et al.*, 2002) resistant to the masticatory forces (Blanton & Biggs, 1969; Schumacher, 1997). The low tensile stress on the floor and high tensile stress at lateral wall, confirm that resultant occlusal forces of the masseter muscle contraction is non-uniformly distributed through the zygomatic pillar.

First molar is considered the key occlusion and has a favorable anatomical functional relationship with the

zygomatic alveolar crest and ZP (Atkinson, 1951). Previously FEA confirmed that first molar occlusal relationship can influence the stress distribution to the zygomatic alveolar crest (Gross *et al.*, 2001; Cattaneo *et al.*). This factor may cause significant impacts for the success or failure of orthodontic treatment, anchorage implants (Benzing *et al.*, 1995; Clelland *et al.*, 1995) and placement of prosthesis (Kregzde, 1993; Benzing *et al.*).

Stress, due to resultant occlusal forces of the masseter muscle contraction, is mainly supported by the zygomatic bone, and distributed predominantly through the zygomatic pillar, non-uniformly, from alveolar process to the superior orbit contour. The stress distribution presented by this study contributes to better understanding in functional morphology of human zygomatic pillar. Thus, these findings can be applied in questions involving the human skull morphology that can be useful in clinical practice.

ACKNOWLEDGEMENTS

The authors are thankful to CNPq (National Counsel of Technological and Scientific Development) for financial support and the Center for Information Technology "Renato Archer" (Campinas, Brazil) for technical and scientific support.

PRADO, F. B.; NORITOMI, P. Y.; FREIRE, A. R.; ROSSI, A. C.; NETO, F. H. & CARIA, P. H. F. Distribución de la tensión en el pilar cigomático humano usando análisis de elementos finitos tridimensional. *Int. J. Morphol.*, 31(4):1386-1392, 2013.

RESUMEN: El objetivo de este artículo fue analizar la distribución de la tensión en el pilar cigomático humano durante la contracción del músculo masetero utilizando análisis de elementos finitos tridimensionales. Un modelo de tres dimensiones de dientes del hemicráneo facial fueron producidos sobre la base de datos de CT-scan. Se utilizó como modelo un cráneo adulto de sexo masculino con la integridad de la anatomía estructural. Fuerzas musculares se aplicaron en el origen de los ascensores de los músculos de la mandíbula y soportes se aplicaron a la superficie oclusal del primer y segundo molar para simular una carga masticatoria y estimular el pilar cigomático. Condiciones de simetría se colocaron en el plano mediano. Se utilizaron restricciones en los planos superior y posterior. El análisis de las tensiones equivalentes von-Mises y máximo director se realizó a través del campo de esfuerzos a lo largo del pilar cigomático. Fue representada la concentración de esfuerzos en el proceso alveolar, hueso cigomático, proceso frontal y temporal del hueso cigomático y el

arco superciliar. La línea de tensión indica la distribución de la tensión del maxilar hacia el hueso frontal y temporal. Las tensiones se produjeron debido a las fuerzas oclusales resultantes, que se apoyan principalmente por el hueso cigomático, distribuidas de manera no uniforme y sobre todo a través del pilar cigomático. Este estudio ha contribuido a una mejor comprensión de la distribución de la tensión en el pilar cigomático para entender la influencia de la masticación sobre la morfología de este pilar y ser de utilidad en la práctica clínica.

PALABRAS CLAVE: Biomecánica; Cráneo; Análisis de elementos finitos.

REFERENCES

- Atkinson, S. R. The mesio-buccal root of the maxillary first molar. *Am. J. Orthod.*, 38:642-52, 1951.
- Benzing, U. R.; Gall, H. & Weber, H. Biomechanical aspects of two different implant-prosthetic concepts for edentulous maxilla. *Int. J. Oral Maxillofac. Implants*, 10(2):188-98, 1995.
- Blaney, S. P. Why paranasal sinuses? *J. Laryngol. Otol.*, 104(9):690-3, 1990.
- Blanton, P. L. & Biggs, N. L. Eighteen hundred years of controversy: the paranasal sinuses. *Am. J. Anat.*, 124(2):135-47, 1969.
- Cattaneo, P. M.; Dalstra, M. & Melsen, B. The transfer of occlusal forces through the maxillary molars: a finite element study. *Am. J. Orthod. Dentofacial Orthop.*, 123(4):367-73, 2003.
- Chalk, J.; Richmond, B. G.; Ross, C. F.; Strait, D. S.; Wright, B. W.; Spencer, M. A.; Wang, Q. & Dechow, P. C. A finite element analysis of masticatory stress hypotheses. A finite element analysis of masticatory stress hypotheses A finite element analysis of masticatory stress hypotheses. *Am. J. Phys. Anthropol.*, 145(1):1-10, 2011.
- Clelland, N. L.; Lee, J. K.; Binbent, O. C. & Brantley, A. A three dimensional finite element stress analysis of angled abutments for an implant placed in the anterior maxilla. *J. Prosthodont.*, 4(2):95-100, 1995.
- Endo, B. Distribution of stress and strain produced in the human facial skeleton by the masticatory force. *J. Anthropol. Soc. Nippon*, 73(4):123-36, 1965.
- Endo, B. A biomechanical study of the human facial skeleton by means of strain-sensitive lacquer. *Okajimas Folia Anat. Jpn.*, 42(4):205-17, 1966a.
- Endo, B. Experimental studies on the mechanical significance of the form of the human facial skeleton. *J. Fac. Sci. Univ. Tokyo*, 3:1-101, 1966b.
- Gross, M. D.; Arbel, G. & Hershkovitz, I. Three-dimensional finite element analysis of the facial skeleton on simulated occlusal loading. *J. Oral Rehabil.*, 28(7):684-94, 2001.
- Herring, S. W. Masticatory muscles and the skull: a comparative perspective. *Arch. Oral Biol.*, 52(4):296-9, 2007.
- Hilloowala, R. & Kanth, H. The transmission of masticatory forces and nasal septum: structural comparison of the human skull and Gothic cathedral. *Cranio*, 25(3):166-71, 2007.
- Huiskes, R. & Chao, E. Y. A survey of finite element analysis in orthopedic biomechanics: The first decade. *J. Biomech.*, 16(6):385-409, 1983.
- Hylander, W. L. & Johnson, K. R. *In vivo bone strain patterns in the craniofacial region of primates*. In: McNeill, C. (Ed.). *Science and Practice of Occlusion*. Hanover Park, Quintessence Publishing, 2000. p.170.
- Hylander, W. L.; Picq, P. G. & Johnson, K. R. Masticatory-stress hypotheses and the supraorbital region of primates. *Am. J. Phys. Anthropol.*, 86(1):1-36, 1991.
- Kregzde, M. A method of selecting the best implant prosthesis design option using three-dimensional finite element analysis. *Int. J. Oral Maxillofac. Implants*, 8(6):662-73, 1993.
- Kupczik, K.; Dobson, C. A.; Fagan, M. J.; Crompton, R. H.; Oxnard, C. E. & O'higgins, P. Assessing mechanical function of the zygomatic region in macaques: validation and sensitivity testing of finite element models. *J. Anat.*, 210(1):41-53, 2007.
- Lanyon, L. E. & Rubin, C. T. *Functional adaptation in skeletal structures*. In: Hildebrand, M.; Bramble, D. M.; Liem, K. F. & Wake, D. B. (Eds.). *Functional vertebrate morphology*. Cambridge, Harvard University Press, 1985. pp.1-25.
- Oyen, O. J.; Melugin, M. B. & Indresano, A. T. Strain gauge analysis of the frontozygomatic region of the zygomatic complex. *J. Oral Maxillofac. Surg.*, 54(9):1092-96, 1996.
- Pavalko, F. M.; Norvell, S. M.; Burr, D. B.; Turner, C. H.; Duncan, R. L. & Bidwell, J. P. A model for mechanotransduction in bone cells: the loadbearing mechanosomes. *J. Cell. Biochem.*, 88(1):104-12, 2003.
- Prado, F. B.; Rossi, A. C.; Freire, A. R. & Caria, P. H. F. The application of finite element analysis in the skull biomechanics and on Dentistry. *Indian J. Dent. Res.*, 2013 (In Press).
- Preuschoft, H.; Witte, H. & Witzel, U. Pneumatized spaces, sinuses and spongy bones in the skulls of primates. *Anthropol. Anz.*, 60(1):67-79, 2002.
- Prossinger, H. & Bookstein, F. L. Statistical estimators of frontal sinus cross section ontogeny from very noisy data. *J. Morphol.*, 257(1):1-8, 2003.

Richmond, B. G.; Wright, B. W.; Grosse, I.; Dechow, P. C.; Ross, C. F.; Spencer, M. A. & Strait, D. S. Finite element analysis in functional morphology. *Anat. Rec. A Discov. Mol. Cell. Evol. Biol.*, 283(2):259-74, 2005.

Ross, C. F. In vivo function of the craniofacial haft: the interorbital "pillar". *Am. J. Phys. Anthropol.*, 116(2):108-39, 2001.

Schumacher, G. H. *Principles of skeletal growth*. In: Dixon, A. D.; Hoyte, D. A. N. & Rönnig, O. (Eds.). *Fundamentals of craniofacial growth*. Boca Raton, CRC Press, 1997. pp.1-21.

Shetty, P.; Hegde, A. M. & Rai, K. Finite element method-an effective research tool for dentistry. *J. Clin. Pediatr. Dent.*, 34(3):281-5, 2010.

Sicher, H. & DuBrul, E. L. *Oral Anatomy*. 5a ed. Saint Louis, Ishiyaku EuroAmerica, 1970.

Silva, M. J.; Brodt, M. D. & Hucke, W. J. Finite element analysis of the mouse tibia-estimating endocortical strain during three-point bending in SAMP6 osteoporotic mice. *Anat. Rec. A Discov. Mol. Cell. Evol. Biol.*, 283(2):380-90, 2005.

Strait, D. S.; Grosse, I. R.; Dechow, P. C.; Smith, A. L.; Wang, Q.; Weber, G. W.; Neubauer, S.; Slice, D. E.; Chalk, J.; Richmond, B. G.; Lucas, P. W.; Spencer, M. A.; Schrein, C.; Wright, B. W.; Byron, C. & Ross, C. F. The structural rigidity of the cranium of Australopithecus africanus: implications for diet, dietary adaptations, and the allometry of feeding biomechanics. *Anat. Rec. (Hoboken)*, 293(4):583-93, 2010.

Strait, D. S.; Weber, G. W.; Neubauer, S.; Chalk, J.; Richmond, B. G.; Lucas, P. W.; Spencer, M. A.; Schrein, C.; Dechow, P. C.; Ross, C. F.; Grosse, I. R.; Wright, B. W.; Constantino, P.; Wood, B. A.; Lawn, B.; Hylander, W. L.; Wang, Q.; Byron, C.; Slice, D. E. & Smith, A. L. The feeding biomechanics and dietary ecology of Australopithecus africanus. *Proc. Nat. Acad. Sci. U. S. A.*, 106(7):2124-9, 2009.

Tanne, K.; Yoshida, S.; Kawata, T.; Sasaki, A.; Knox, J. & Jones, M. L. An evaluation of the biomechanical response of the tooth and periodontium to orthodontic forces in adolescent and adult subjects. *Br. J. Orthod.*, 25(2):109-15, 1998.

Turner, C. H. Three rules for bone adaptation to mechanical stimuli. *Bone*, 23(5):399-407, 1998.

Wroe, S.; Ferrara, T. L.; McHenry, C. R.; Curnoe, D. & Chamoli, U. The craniomandibular mechanics of being human. *Proc. Biol. Sci.*, 277(1700):3579-86, 2010.

Correspondence to:
Prof. Dr. Felipe Bevilacqua Prado
Department of Morphology - Anatomy area
Piracicaba Dental School
State University of Campinas
Av Limeira, 901, PO Box 52
Piracicaba, São Paulo
BRAZIL

Email: fprado@fop.unicamp.br

Received: 23-06-2013

Accepted: 02-11-2013